Laser Physics, Vol. 15, No. 2, 2005, pp. 328–333.

Measurements of Chirp-Induced Frequency Shift in High-Order Harmonic Generation in Xenon

F. Giammanco[1], A. Pirri[1], F. Brandi[2, *], M. Barkauskas[2], and W. Ubachs[2]

[1] *Department of Physics, University of Pisa, Via F. Buonarroti 2, 56127 Pisa, Italy*
[2] *Laser Center, Department of Physics and Astronomy, Vrije Universiteit, De Boelelaan 1081, 1081 HV Amsterdam, The Netherlands***
*e-mail: brandi@df.unipi.it
**URL: http://www.nat.vu.nl/~laser

Received August 26, 2004

Abstract—A precise metrology experiment on the ninth harmonic generated in the nonperturbative regime in xenon is presented. Harmonic generation is performed with a 300-ps 4-GW narrowband tunable laser, and well-calibrated atomic resonances are used as a frequency markers in the extreme ultraviolet, enabling an absolute frequency calibration at the 10^{-6}–10^{-7} level. A harmonic frequency is observed that deviates from the expected integer multiple of the fundamental frequency. This frequency shift is found to increase with gas density starting from negative values, i.e., redshift, at a low gas density. Possible sources of the observed frequency shift are critically discussed. The increase of the frequency shift toward high gas densities is consistent with self-phase modulation of the fundamental beam due to the presence of free electrons in the interaction region that are generated via multiphoton ionization, while the observed redshift toward lower gas densities may be attributable to plasma-dynamics effects.

1. INTRODUCTION

An outstanding issue in high-order harmonic generation (HHG) in gases, one which has attracted attention in recent years, is the measurement and control of the frequency spectrum of the harmonic radiation. HHG is a coherent process, and the frequency characteristics of the generated radiation are determined by the interplay of several factors: the frequency spectrum and chirp of the fundamental pulse, the self-phase modulation of the fundamental pulse interacting with the nonlinear gaseous medium, and the intrinsic chirp phenomenon in the harmonic-generation process. These phenomena give rise to a broadening of the harmonic frequency spectrum as well as to an effective shift in the central frequency of the harmonics with respect to the integer multiples of the fundamental frequency.

The assessment of chirp-induced shifts in HHG is important in many applications in physics and chemistry when the radiation produced, preferably narrowband and tunable, is being used as a spectroscopic tool. The chirp process in HHG is found to depend largely on the specific conditions in the interaction region, namely, on the intensity and duration of the fundamental laser pulses, the gas density, and the degree of plasma formation.

When fs pulses are used in HHG, nonadiabatic single-atom effects related to the effective change in the electric-field amplitude during a laser period play an important role [1] in shaping the spectral profile of the harmonic pulses. Such an effect scales with the inverse of the time duration of the fundamental laser pulse [2]; it is much less pronounced when ns and ps pulses are used.

Collective effects are related to self-phase modulation (SPM) of the fundamental pulses induced by the sudden change of the refractive index during the laser–matter interaction. SPM due to the Kerr effect of neutrals gives rise to a frequency *redshift* in the rising edge and *blueshift* in the falling edge of the pulse. When the laser intensity is high enough to photoionize the gas, a plasma is formed and the index of refraction is dominated by free electrons, as described by Yablonovitch [3]. The increase in the free-electron density that occurs during the laser pulse induces a frequency blueshift. When relatively long pulses are used (>few ps), the plasma dynamics starts to play an important role. Free electrons can escape the focal region [4] or recombine with ions, thus leading to a decrease in the electron density during the laser–plasma interaction and, hence, can contribute to a frequency redshift.

Recently, harmonic generation in the nonperturbative regime was demonstrated to be feasible at pulse durations as long as 300 ps [5] using a novel laser system developed at the Laser Center of the Vrije Universiteit (Amsterdam) [6]. The same setup is now employed to quantitatively address chirp-induced shifts in the ninth harmonic generated in xenon. The relatively long pulse duration (10^3–10^4 times longer than in experiments employing fs pulses), the associated narrow bandwidth, and the possibility of continuous wavelength scanning allow for precision metrology studies of the chirp phenomenon using well-calibrated atomic resonances as frequency markers in the extreme ultra-

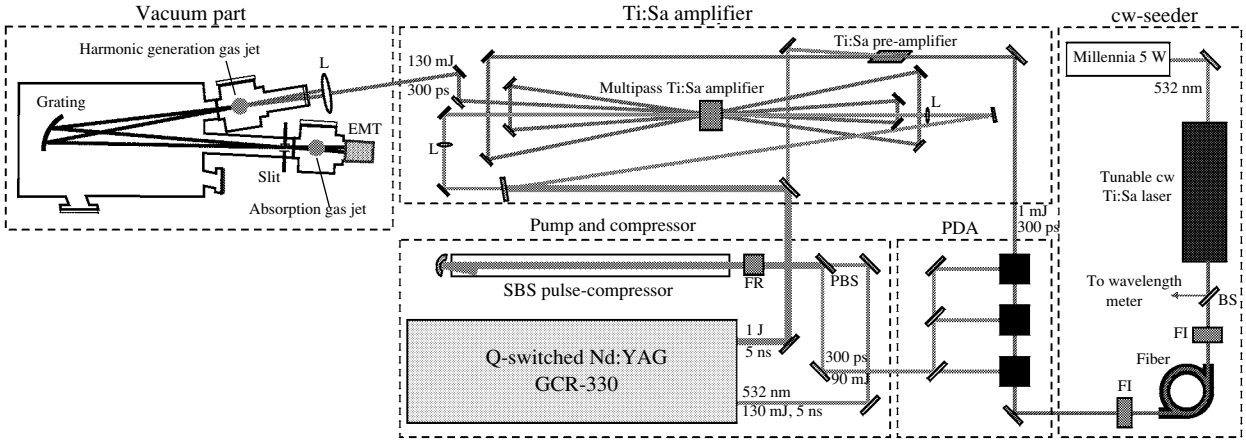

Fig. 1. Schematic of the experimental apparatus.

violet. Previously, in studies employing femtosecond pulses, fractional frequency shifts $\Delta\nu_q/\nu_q$ on the order of a few percent were observed [7]. Under conditions of longer pulses, the rate of change of the refractive index is much smaller and, hence, the expected chirp is much less. However, the unique metrology setup in our laboratory, which involves a continuously tunable high-power laser source, allows for registration of small fractional frequency shifts within 10^{-6}–10^{-7}. The harmonic frequency shift is found to be an increasing function of the gas density, indicating the effect of free electrons created by multiphoton ionization. At a low gas density, a redshift is observed and is attributed to plasma-dynamics effects during the relatively long time (300 ps) of the fundamental pulse.

2. EXPERIMENTAL APPARATUS

A schematic of the experimental apparatus is shown in Fig. 1. The output frequency of the combined set of lasers and amplifiers is determined by that of the continuous wave Ti:Sa ring laser. It may be scanned mode-hop-free over a limited range of about 1 cm^{-1}, and it can be set at wavelengths between 750 nm and 800 nm without changing the mirror set. The pulsed-dye amplifier (PDA), which runs on LDS-765 (Exciton) dye, allows for coverage of the wavelength range 750–795 nm. The three-stage PDA, which is pumped by compressed pulses (300 ps, 532 nm) from a 1-m-long Brillouin cell filled with clean water [6], determines the spectral and temporal properties of the energetic near-infrared (NIR) laser pulses: they follow the time duration of the pump pulse and have a nearly Fourier-transform-limited bandwidth (~1.5 GHz). A 1-cm-long Brewster-cut Ti:Sa crystal with a diameter of 1 cm is used in the multipass amplifier to yield a maximum NIR pulse-output energy of 130 mJ. The actual energy of the pulses used for HHG is controllable by means of a variable attenuator formed by a half-wave plate and a thin-film polarizer. The spatial beam quality is investigated using a beam-profile analyser (DataRay, Model: WinCamD), and a propagation factor of $M^2 = 1.2$ is found, indicating that the spatial characteristics of the energetic near-infrared pulses generated by the laser system are almost entirely determined by the TEM_{00} cw seeding beam. The diameter of the NIR beam at the output of the amplifier is about 6 mm. In order to achieve the high intensities needed for HHG, a relatively strong focusing is employed using an anti-reflection-coated lens with a 15-cm focal length and allowing for a focal-spot intensity of about 5×10^{13} W/cm^2.

Harmonics are produced in a freely expanding pulsed xenon gas jet at about 0.5 mm downstream from the orifice of a piezo-electric pulsed valve that was home-built following the design of [8] with a 1-mm opening diameter. The laser propagation length through the gas is about 1 mm. Both the backing pressure for the valve and the running pressure in the differentially pumped vacuum chamber were monitored and were found to be linearly dependent for a backing pressure in the range (0.7–1.6) bar with a running pressure in the vacuum chamber in the range (10^{-6}–10^{-5}) mbar. This corroborates the finding reported in [8], namely, that the gas flow varies linearly with the gas backing pressure. In view of this, the backing pressure is assumed to be, in a good approximation, a relative measure for the density in the focal region. With a voltage of about 230 V on the piezo-electric valve, the gas density in the interaction region is estimated to be around 10^{17} cm^{-3} (a local gas pressure of few mbar) for a backing pressure of 1 bar.

The generated harmonics are dispersed with a gold-coated normal incidence grating and detected with an electron-multiplier tube. In Fig. 2, the harmonic spectrum generated in xenon with an intensity of $I = 4 \times$

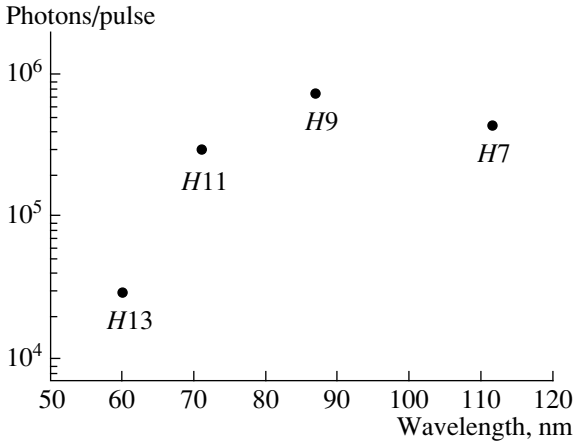

Fig. 2. Harmonic yield obtained with a laser intensity of 4×10^{13} W/cm^2; *Hq* denotes the harmonic of order *q*.

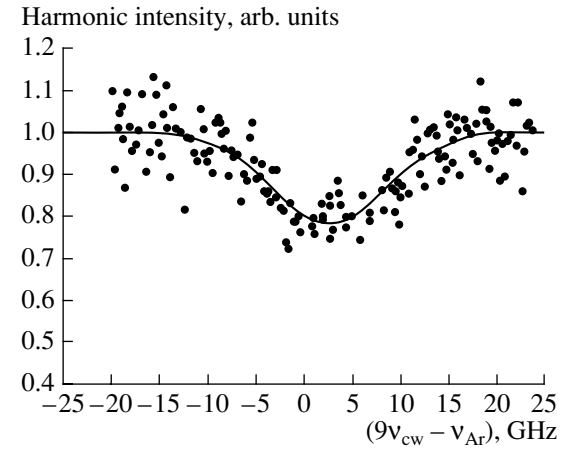

Fig. 3. Frequency metrology on the generated harmonics: spectral recording of the $(3p^6\ ^1S_0 \longrightarrow 3p^5 3d'[3/2]_1)$ transition in Ar at 86.7 nm (λ_{cw} = 780 nm) measured by linear absorption of the ninth harmonic produced in Xe with 1.1-bar backing pressure and $I = 4.3 \times 10^{13}$ W/cm^2.

10^{13} W/cm^2 is shown. The HHG cutoff energy is given approximately by $I_p + 3U_p$, where I_p is the ionization potential of the atom and U_p [eV] = $9.33 \times 10^{-14} I$ [W/cm^2] λ^2 [μm] is the ponderomotive energy of the photoelectrons. Under the present experimental conditions (I_p(Xe) = 12.1 eV, λ = 0.78 μm), the cutoff order for the produced harmonics is 12, which is in good agreement with the experimental findings.

Of crucial importance for the experiments reported here is the determination of frequencies, both for the fundamental and the harmonics. For the fundamental frequency, accurate wavelength determinations were performed using a wavelength meter (ATOS, Model: LM-007) equipped with four etalons to measure the seeding frequency ν_{cw} of the cw Ti:Sa laser. In the course of the investigations, the wavelength meter was recalibrated several times in measurements on the I_2 hyperfine components [9], and each time the calibration was found within 50 MHz, thus setting an uncertainty limit on ν_{cw}.

In a pulse-amplification system using fluorescent dyes, the central frequency of the output pulses is known to undergo effective shifts with respect to the seed frequency. This is a chirp phenomenon originating from the time-dependent gain in the dye amplifier [10, 11]. The effective net shift between the seeding frequency ν_{cw} and the central frequency of the amplifier output pulses ν_1 can be determined from transmission profiles of both beams through an etalon and is found to be less than 100 MHz [12].

With pulses of 300-ps duration, it is not possible to determine the time-dependent frequency excursions during the pulse, as was demonstrated for ns pulses in [13]. Thus, to account for the frequency chirp in the amplification process, the actual central frequency of the fundamental pulses used for the HHG experiment is assumed to be equal to ν_{cw}, thereby conservatively estimating the uncertainty at 200 MHz.

3. EXPERIMENTAL METHOD AND RESULTS

In order to determine the shifts that result from chirp in the HHG process, the expected harmonic frequencies $q\nu_{cw}$ will be compared with the actual observed frequencies in the extreme ultraviolet. For this purpose, absorption spectra of the well-calibrated $(3p^6\ ^1S_0 \longrightarrow 3p^5 3d'[3/2]_1)$ atomic transition in Ar at a frequency ν_{Ar} = 3458611.8 GHz, or roughly 86.7 nm (λ_{cw} = 780 nm), were measured. The level energies of the electronically excited states of argon are all known with high relative accuracy, and it is only the level energy of the ground state that introduces uncertainty. Via the measurement of the $(3p^6\ ^1S_0 \longrightarrow 3p^5 4s'[1/2]_1)$ transition made by Velchev *et al.* [14], the absolute accuracy of all VUV transitions in Ar [15] is established to be within 1.5 GHz. In particular, for the presently used transition in Ar, a lower uncertainty of about 0.3 GHz can be inferred using the data reported in Table 6 in [15].

Figure 3 shows an example of a recorded absorption spectrum in Ar of the ninth harmonic generated in xenon. The resonances are plotted on a scale of the frequency $9\nu_{cw} - \nu_{Ar}$ as derived from the wavelength meter ν_{cw} and the transition frequency in the absorbing gas ν_{Ar}. The solid line presents the result of a least-squares fit to the data points with a Gaussian profile; its center then determines the frequency shift associated with the HHG process. Note that a redshift in the present graph represents an actual blueshift of the harmonic frequency and *vice versa*. The width of the absorption resonances is a combined effect of Doppler broadening in

the free gas jet and the bandwidth of the harmonic. However, most absorption profiles are recorded with about 50% absorption; thus, saturation effects are not negligible and a systematic investigation of the broadening of the spectral profile has not yet been performed. For those measurements below saturation, a 15-GHz width was observed for the argon resonance at the ninth harmonic. Assuming an effective opening angle for the free jet expansion of $\theta = 40°$ (typical for a solenoid valve used for the absorbing gas jet) and a gas speed (v) of 400 m/s for Ar, the Doppler contribution, which is given by $\Delta\nu_D = (v/c)\nu \sin\theta$, is 3 GHz at the ninth harmonic.

The absorption spectra of the argon resonances are recorded using the ninth harmonic generated in xenon at different values of the gas backing pressure of the piezo-electric valve. The frequency shift of the harmonic radiation is determined as $\Delta\nu_9 = \nu_{Ar} - 9\nu_{cw}$. In Fig. 4, the measured shifts of the ninth harmonic generated in Xe at a peak intensity of 1.3×10^{13} W/cm^2 and 4.3×10^{13} W/cm^2 are presented along with the statistical errors resulting from the fitting procedure. The error in the absolute value of the frequency shifts reported in Fig. 4 arises from the uncertainty in the transition frequency (0.3 GHz) and in the metrology on the fundamental frequency (0.2 GHz) and is estimated at 1.8 GHz.

The ionization in the interaction zone, where the harmonics are generated, was further characterized as well. The multiphotoionization saturation intensity for xenon under our experimental conditions, which was calculated using the closed-form equation derived in [16], is I_s^{cal} (Xe) = 1.1×10^{13} W/cm^2. Measurements on the ion yield *versus* laser intensity, performed with a grid placed downstream the gas jet, result in saturation intensities of I_s^{exp} (Xe) $\leq 10^{13}$ W/cm^2, in good agreement with the calculated values. Thus, full ionization is achieved during the pulse at the laser intensities used in the experiments.

4. DISCUSSION

The central observations of the present study (shown in Fig. 4) are the frequency redshift with a magnitude of up to 6 GHz at low gas densities and the almost linear increase in the frequency shift with gas density. These phenomena can be ascribed to plasma formation and dynamics during the fundamental laser pulse, as will be explained in the following.

Chirp phenomena related to collective or macroscopic effects are due to the rate of temporal change of the refractive index in the nonlinear medium. Based on this effect of SPM of the incident laser pulse, a chirp is imposed on all of the harmonics.

High-order harmonic generation is accompanied by ionization of the medium, resulting in a fully ionized plasma at the highest intensities. In a plasma, the index

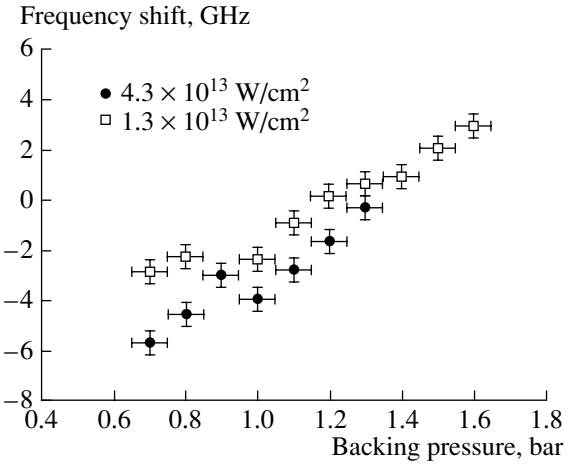

Fig. 4. Frequency shifts of the ninth harmonic generated in Xe at a peak intensity of 1.3×10^{13} W/cm^2 and 4.3×10^{13} W/cm^2.

of refraction is governed by the free electrons: $n^{el}(\nu, z, t) = [1 - (\nu_p(z, t)/\nu)^2]^{1/2}$, where $\nu_p^2 = e^2 N_e(z, t)/4\pi^2 m_e \epsilon_0$ is the time-dependent electronic plasma frequency and $N_e(z, t)$ is the electron density. Plasma formation causes a blueshift in the harmonic frequencies, because $N_e(z, t)$ increases during the HHG process. At electron densities typical of HHG experiments ($N_e \ll 10^{21}$ cm^{-3}), the plasma frequency is much smaller than the laser frequency, and the blueshift in the harmonic radiation can be estimated as

$$\Delta\nu_q^{el}(t) = \frac{qe^2}{8\pi^2 c m_e \epsilon_0 \nu_1} \int^L \frac{\partial N_e(z, t)}{\partial t} dz, \qquad (1)$$

where the integration is over the propagation length in the medium. Under conditions of saturation of the photoionization process and assuming a homogeneous medium, the rate $\partial N_e(z, t)/\partial t$ can be approximated by N_0/τ_{eff}, where N_0 is the initial atomic density and τ_{eff} is the effective time for achieving complete ionization for laser intensities above the saturation intensity. This predicts a blueshift that is linearly dependent on the gas density in the focal region:

$$\Delta\nu_q^{el} = \frac{qe^2 L}{8\pi^2 c m_e \epsilon_0 \nu_1} \frac{N_0}{\tau_{eff}}. \qquad (2)$$

Wahlström *et al.* [7] experimentally observed blueshifts in harmonics from a 150-fs fundamental pulse that where consistent with this effect of plasma formation.

An estimate of the blueshift due to the plasma can be made using Eq. (2) with $L = 1$ mm, $\nu_1 = 4 \times 10^{14}$ Hz, and $\tau_{eff} \sim 100$ ps, which leads, for the ninth harmonic generated in a fully ionized gas of pressure 3 mbar ($N_0 \sim 10^{17}$ cm^{-3}), to a shift of $\Delta\nu_9^{el} \sim 3$ GHz. This is of

the same order as the shifts observed experimentally, thus confirming the presence of plasma-induced chirp in HHG.

As an increase in the electron density can induce a blueshift in the generated harmonics, so a decrease in N_e will result in a frequency redshift, as follows from Eq. (1). At first glance, recombination seems to be a good candidate for explaining the origin of electron losses from the interaction region. In a relatively dense and cold plasma, as in our case (i.e., an electron temperature T_e on the order of 1 eV and N_e of about 10^{17} cm^{-3}), the recombination is a three-body process. The time constant of three-body recombination, assuming that $N_e = N_i$, where N_i is the ion density, is given by

$$\tau_{\text{rec}} = K\frac{T_e^{9/2}}{N_e^2}, \tag{3}$$

where τ_{rec} is in seconds, T_e is in eV, N_e is in cm^{-3}, and $K = 10^{25}$ (esu) [17]. Although approximated, this formula allows us to implement the main features of three-body recombination under our experimental conditions. First of all, with $T_e = 1$ eV and $N_e = 10^{17}$ cm^{-3}, we obtain $\tau_{\text{rec}} = 10^{-9}$ s, a value that is noticeably longer than the laser-pulse duration. Moreover, τ_{rec} decreases quadratically with the electron density; thus, recombination should enhance the redshift at a higher density, in contrast with the experimental evidence. In addition, one can expect that the electron temperature does not maintain its initial value. In fact, due to electron–ion collisions, the quiver velocity gained by the electrons in the strong laser field is transformed into random motion, i.e., electron heating, thus leading to a further increase in τ_{rec}. Hence, recombination can be excluded as a source of the observed redshift.

It is conceivable that a harmonic redshift can be associated with plasma dynamics. If the laser pulses have sufficiently long duration, electrons have time to escape the focal zone, thus causing n^{el} to grow again. In the present experiment, the fundamental pulses are focused on a spot with a radius of about 15 μm; assuming a 1-eV kinetic energy for the generated photoelectrons, they can fly out of the interaction region in about 25 ps, which is much less then the pulse duration. When substantial ionization occurs already before the peak of the pulse, the electron dynamics can be effective during the harmonic-generation process involving neutral atoms. Once electrons begin to be produced by multiphoton ionization, they expand rapidly until the ion density is less than the threshold for electron trapping, i.e., when the field due to ions forces the electrons to oscillate at the plasma frequency. After total ionization, the electron oscillations are damped by strong Coulomb collisions with ions. Hence, we can infer that a partial departure from plasma neutrality can occur in a short time (tens of ps) compared to the laser pulse duration (300 ps).

An alternative source of a frequency redshift is related to the Kerr effect of neutral atoms, which produces a frequency excursion in the fundamental beam that is given by

$$\Delta\nu^K(t) = -\frac{\nu_1 n_2}{c}\int^L \frac{\partial I(t)}{\partial t}dz, \tag{4}$$

where n_2 is the nonlinear refractive index. When the ionization rate during the pulse is small, SPM due to the Kerr effect will induce an almost symmetric broadening in the frequency spectrum. However, if one assumes that HHG takes place predominantly during the leading edge of the intense laser pulse, the Kerr effect induces a redshift in the harmonic radiation that can be approximated by

$$\Delta\nu_q^K = -\frac{q\nu_1 n_2 I_0 L}{c\tau}. \tag{5}$$

An estimate of the expected frequency redshift due to the Kerr effect can be performed considering the value of the nonlinear refractive index of gases: $n_2(\text{Xe}) \sim 8 \times 10^{-23}$ m^2/W at 1 bar (gas density ~3×10^{19} cm^{-3}) [18]. Using Eq. (5) with $\tau = 300$ ps, $I_0 = 4 \times 10^{13}$ W/cm^2, $L = 1$ mm, and $\nu_1 = 4 \times 10^{14}$ Hz, the shift for the ninth harmonic generated in a jet with a gas pressure of about 10 mbar is $|\Delta\nu_9^K| \sim 12$ MHz. This value is two orders of magnitude smaller than the experimental results; thus, it can be ruled out as a possible source of the observed redshift in HHG with 300-ps pulses.

5. CONCLUSIONS AND OUTLOOK

A high-resolution study of chirp effects in HHG was performed. This was possible thanks to the accurate metrology on the fundamental laser frequency and the high spectral purity of the harmonics. Frequency shifts in the ninth harmonic produced in xenon were measured with an accuracy on a level of 10^{-6}–10^{-7}, thus enabling a careful investigation of the chirp phenomenon in HHG.

At peak laser intensity above the saturation intensity, the distinct effect of plasma formation is demonstrated by a frequency blueshift that is proportional to the gas density. A frequency redshift is observed at a low gas density. Plasma dynamics can induce a frequency redshift that is due to electrons leaving the interaction region during the 300-ps pulse duration. A quantitative study of the full plasma dynamics and the corresponding harmonic generation is at present in progress. However, from an inspection of possible phenomena responsible for the redshift, it seems likely that the electron dynamics can be ascribed to the source of the redshift observed in the harmonic frequency.

The experiments reported show that high-resolution studies of the high-order-harmonics frequency spectrum are possible thanks to the unique characteristics of

continuous wavelength scanning and narrow bandwidth of the XUV laser source built in our laboratory.

ACKNOWLEDGMENTS

A.P. and M.B. thank the European Union for a Marie Curie host site fellowship at LCVU (HPMT-CT-2000-00063). F.G. wishes to thank the Laser Center of Vrije Universiteit for their hospitality. This study is supported by the European Community Integrated Infrastructure Initiative Action (RII3-CT-2003-506350).

REFERENCES

1. M. Lewenstein, P. Saliéres, and A. L'Huillier, Phys. Rev. A **52**, 4747 (1995).
2. H. J. Shin, D. G. Lee, Y. H. Cha, *et al.*, Phys. Rev. A **63**, 053407 (2001).
3. E. Yablonovitch, Phys. Rev. A **10**, 1888 (1974).
4. E. Yablonovitch, Phys. Rev. Lett. **60**, 795 (1988).
5. F. Brandi, D. Neshev, and W. Ubachs, Phys. Rev. Lett. **91**, 163901 (2003).
6. F. Brandi, I. Velchev, D. Neshev, *et al.*, Rev. Sci. Instrum. **74**, 32 (2003).
7. C.-G. Wahlström, J. Larsson, A. Persson, *et al.*, Phys. Rev. A **48**, 4709 (1993).
8. D. Proch and T. Trickl, Rev. Sci. Instrum. **60**, 713 (1988).
9. I. Velchev, R. van Dierendonck, W. Hogervorst, and W. Ubachs, J. Mol. Spectrosc. **187**, 21 (1998).
10. S. Gangopadhyay, N. Melikechi, and E. E. Eyler, J. Opt. Soc. Am. B **11**, 231 (1994).
11. N. Melikechi, S. Gangopadhyay, and E. E. Eyler, J. Opt. Soc. Am. B **11**, 2402 (1994).
12. F. Brandi, PhD Thesis (Vrije Univ., Amsterdam, 2004).
13. K. S. E. Eikema, W. Ubachs, W. Vassen, and W. Hogervorst, Phys. Rev. A **55**, 1866 (1997).
14. I. Velchev, W. Hogervorst, and W. Ubachs, J. Phys. B **32**, L511 (1999).
15. L. Minnhagen, J. Opt. Soc. Am. **63**, 1185 (1973).
16. B. Chang, P. R. Bolton, and D. N. Fittinghoff, Phys. Rev. A **47**, 4193 (1993).
17. Ya. B. Zel'dovich and Yu. P. Raizer, *Physics of Shock Waves and High-Temperature Hydrodynamic Phenomena*, 2nd ed. (Nauka, Moscow, 1963; Academic, New York, 1966, 1967), Vols. 1, 2.
18. E. T. J. Nibbering, G. Grillon, M. A. Franco, *et al.*, J. Opt. Soc. Am. B **14**, 650 (1997).